DESIGN AND ANALYSIS OF DLS STEEL/COMPOSITE THICK-ADHEREND ADHESIVE JOINTS

S Hashim[1], C Berggreen[2], N Tsouvalis[3], D McGeorge[4], I Chirica[5], P Moore[6], S Boyd[7]
J Nisar[1], K Anyfantis[3], K Misirlis[8], E Juin[9]
1. University of Glasgow, Glasgow G12 8QQ UK.
2. Technical University of Denmark, DK-2800 Kgs. Lyngby, Denmark
3. National Technical University of Athens, GR-15773 Zografos, Athens, Greece.
4. Det Norske Veritas, Norway.
5. University 'Dunarea de Jos' of Galati-800008, Romania.
6. TWI, Cambridge CB21 6AL UK.
7. University of Southampton, Southampton SO17 1BJ UK.
8. University of Newcastle upon Tyne, Newcastle, NE1 7RU UK.
9. Centre of Maritime Technologies e.V, 22305, Hamburg Germany.

SUMMARY

The paper describes experimental and numerical techniques to study the structural design and behaviour of thick-adherend DLS joints that are based on steel /steel and steel/composites and epoxy adhesives, with focus on long overlap joints. A standard fabrication method was followed to produce 60 specimens of various dimensions and materials.

Keywords: Bonded joint design, Composite, Lap-shear test, FEA.

INTRODUCTION

Structural adhesives are gaining wider recognition by industry as they offer engineers greater flexibility to achieve economic and technical advantages. In the marine industry there is potential for adhesives in various types of constructions, for example, bonding hybrid thick steel and composite joints, typically 5-10mm. Advantages of composite materials in the marine industry are their corrosive resistant properties, their lightweight characteristics and their potential for fire resistant design. Applications include superstructures for ships and offshore platforms as well as their suitability as a repair method for cracks and corroded areas [1,2]

The lack of a universally applicable criterion for predicting the static load carrying capacity of adhesively bonded joints means that analytical design optimisation of bonded structures is not possible [3-5]. Also, the use of composite materials within bonded joints further complicates the analysis of these joints due to their inherent orthotropic material properties including weakness of the matrix resin. One of the most widely used connections for adhesive bonding is the DLS joint. Although many investigations have been conducted on double strap joints in the configuration of steel as the outer adherend and composite as the inner adherend, the same cannot be said about the reverse situation. These joints could be considerably longer than standard bonded joints which can benefit from having thicker adherends with the effects of extending the shear of the adhesive more effectively within the joint than with thinner adherend due to stiffness limitation. In patch repair for example, the double lap shear (DLS) joints may give good resemblance to a patch repaired crack. Both joint types experience combined stresses of shear and peel at joint ends. This technology is currently used for repair work onboard floating production storage and offloading units (FPSO's). Figure 1 shows resemblance between the two cases where both designs rely on determining the shear stress level in the joint. The figure also shows a typical behaviour of the DLS joint which causes peel and shear stresses at the middle and outer edges of the joint. The behaviour of DLS joints has been widely studied but these

largely apply to thin adherends and short overlap which may not be the case when dealing with DLS joints with long and thick adherend. Adding to complexity is furthermore the complication of bonding layered composites.

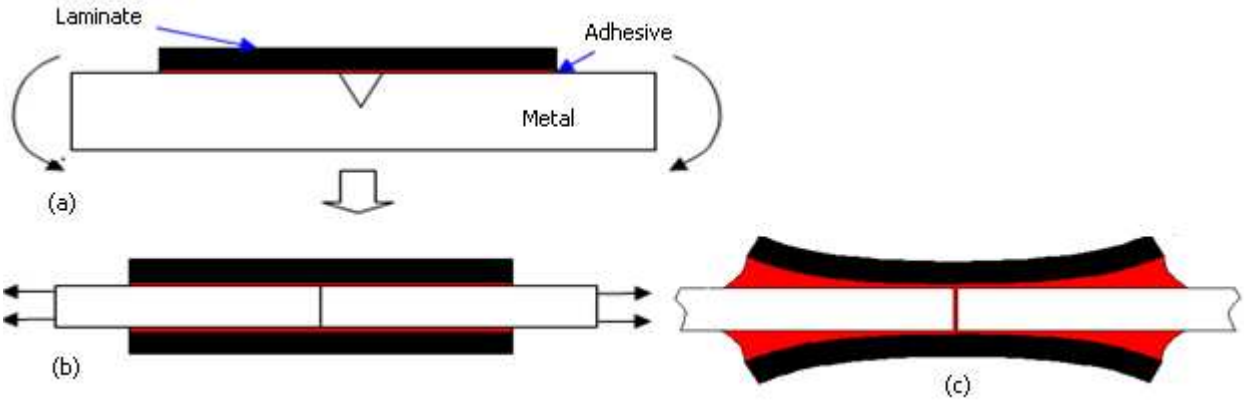

Figure 1. Overlap similarity between (a) a patch repair and (b) a DLS joint and (c) an exaggerated behaviour of the DLS joint.

Toughened epoxy adhesives are often needed for these joints, but the adhesive and its interface remain the weak link, especially in steel/steel and possibly also in steel/CFRP joints. Therefore, it is essential to understand structural behaviour and failure of these joints assuming a good fabrication process is followed. Besides the adhesive and joint geometry, the type of the composite adherend in terms of its stiffness and strength plays an important part in achieving a high bearing load capacity. Additionally, the matrix resin is often the main weakness within bonded composites.

This paper is a joint effort of various partners within the MARSTRUCT Research Network of Excellence on marine structures. The study involves fabrication, testing and numerical analysis undertaken at various institutions (see above affiliations) for benchmarking purposes. The study seeks to provide a guide on the design and fabrication of thick adherend double lap shear joints (DLS), often referred to as butt connections/joints in ship structures including patch repair. The specimens consist of 10 mm steel inner adherend and various outer adherend materials including 0/90 WR GFRP and 0/90 UD CFRP laminates and steel. The focus here is on steel/CFRP joint due to availability of test data. The thickness of the outer adherend varies from 3 mm to 6 mm. Shear overlaps of 25-200 mm were considered. The overall objectives are (i) to assess the quality of the standard fabrication method, (ii) to determine joint strength and overlap plateau for various specimens with a range of material combinations and (iii) to understand aspects of failure and design of the DLS joint under quasi-static loading. The paper presents the experimental and numerical details with key conclusions.

EXPERIMENTAL PROGRAMME

Fabrication

The bonding process will typically require several operations including surface roughening, degreasing, marking, adhesive application, positioning and clamping, curing and finally removal from the clamps. The bonding process was set out taking long term bond performance into consideration. The bonding surfaces of the steel components were prepared by grit blasting or heavy abrasion by silicon carbide/emery paper. Teflon sheeting was applied to one end of each steel adherend to prevent end-to-end joints so that all loading was transferred through shear along the straps rather than a tensile load between the steel adherends. The bonding surfaces of the straps were prepared by light abrasion using 120 grit silicon carbide paper. All bonding

surfaces were cleaned using a cleaning and degreasing agent. Markings were put on the steel bars and straps to ensure correct fit-up of the joint when being bonded.

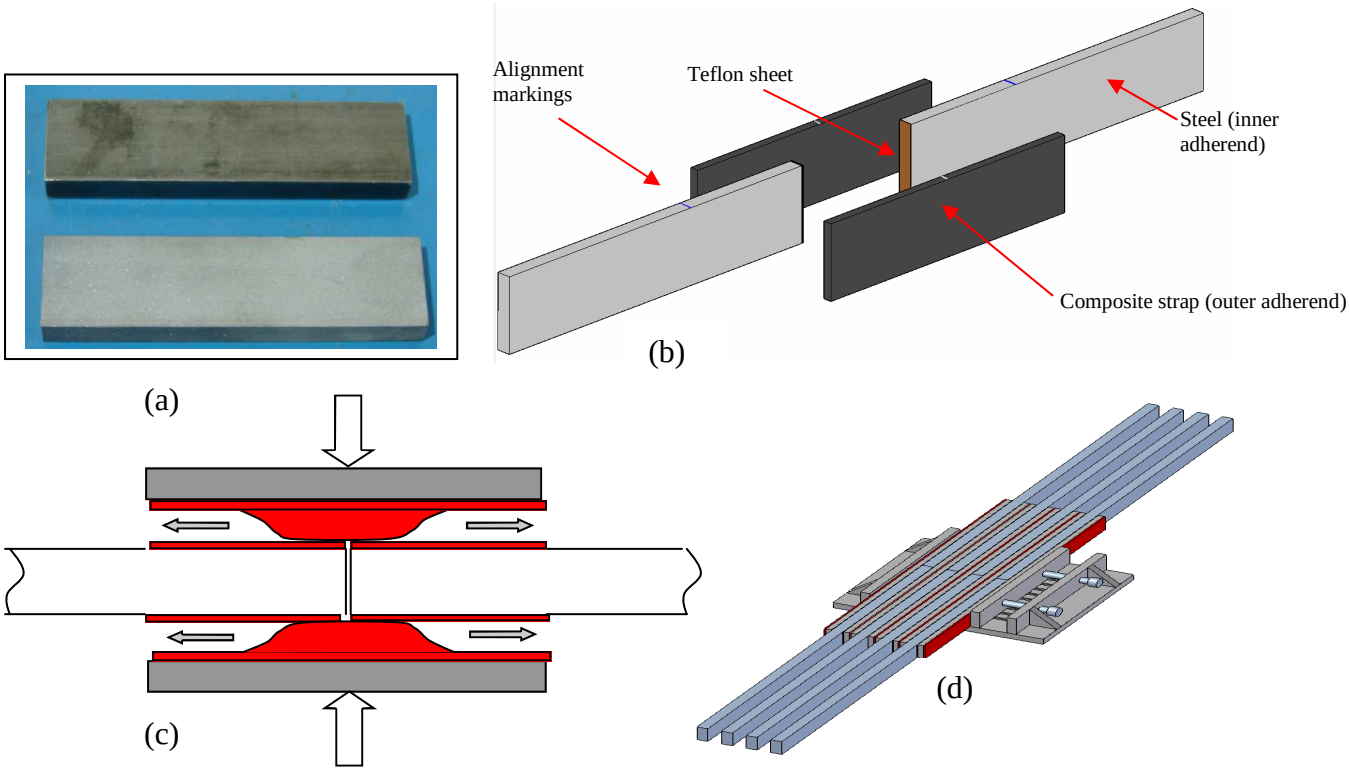

Figure 2. Aspects of the adhesive bonding processes – (a) surface preparation, (b) marking and alignment, (c) adhesive application and (d) clamping and curing.

The adhesive used was Araldite 2015 (HUNTSMAN), a two-part toughened epoxy adhesive which was mixed and applied by spatula in two stages. The first stage is to prime the surfaces with a thin layer of adhesive. The second stage is to apply more adhesive and spread the excess amount. Finally, to close the joint such that the entire bondline is filled with adhesive as shown in Figure 2. The clamping jigs were sprayed with Teflon spray to prevent the specimens sticking. The clamps were tightened evenly to give a uniform thickness of the adhesive layer – typically 0.5mm. The curing of the adhesive joints was done for 1 hour in an oven at 85^{o} C. Finally, any excess adhesive from the joint was mechanically removed so that there were no effective adhesive fillets within the double lap joint. It was assumed that this would reduce variability and make modelling of the specimen configurations easier.

The bonded specimens, all 25 mm wide, incorporated various design and materials parameters including overlap length ranging from 25 mm to 200 mm as well as various materials combinations. 60 specimens were fabricated, designated and tested at various institutions as part of the benchmarking. The designations for the specimens specify “overlap length/strap thickness & strap material/ number of specimen & fabrication site”. For example a specimen designation of 200/6C/G1 refers to 200 mm overlap/6mm thick CFRP straps/specimen no. 1 fabricated in Glasgow. All inner adherends were 10 mm thick and based on steel.

Mechanical testing

The bonded specimens were then tested to destruction under monotonic loading on universal tensile testing machines at ambient temperature. Besides failure loads, both strain and displacement values were recorded. Figure 3 shows the test arrangement including position of the strain gauges and details of the DLS joints.

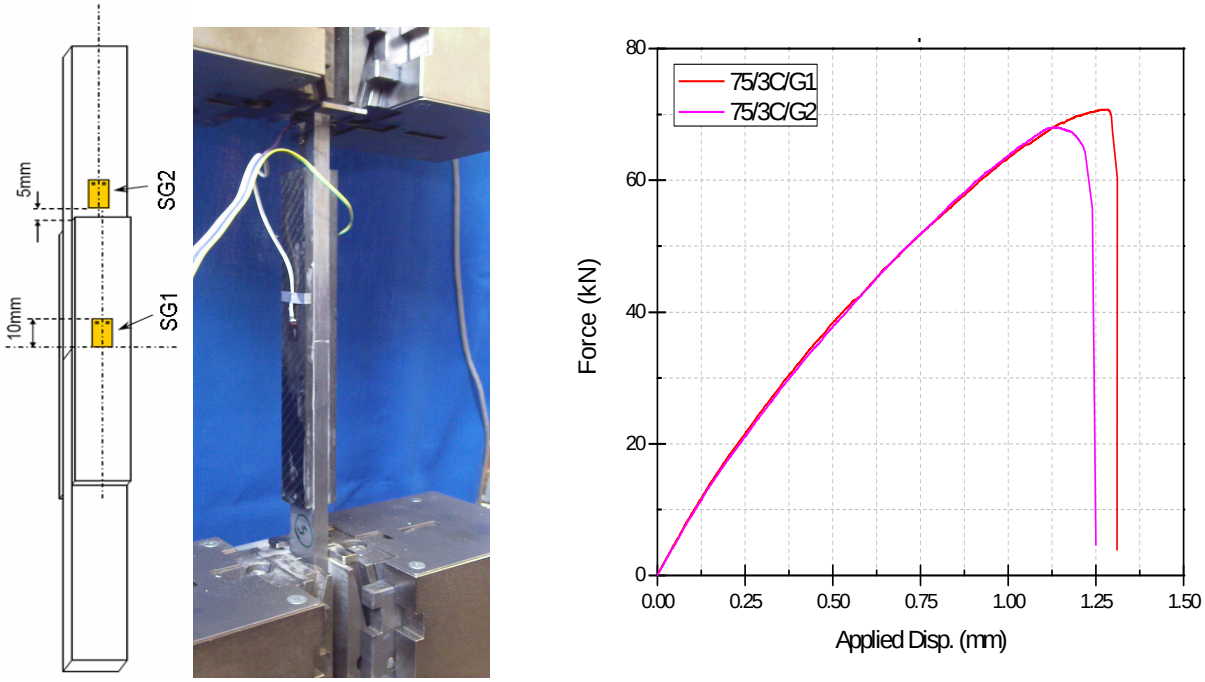

Figure 3. Test set-up and typical load-deflection curves.

Figure 4 shows the trend of failure load versus overlap length with reference to steel/steel and steel/CFRP specimens only. From the figure the following remarks may be made:

- the failure load seems to be proportional to the overlap length up to 100 mm overlap where a plateau is reached. An approximate lines are plotted in relation to steel/steel is steel/CFRP joints
- steel/steel joints exhibited a slightly higher strength than steel/CFRP joints
- steel/GRP joints exhibit significantly lower strength than the rest

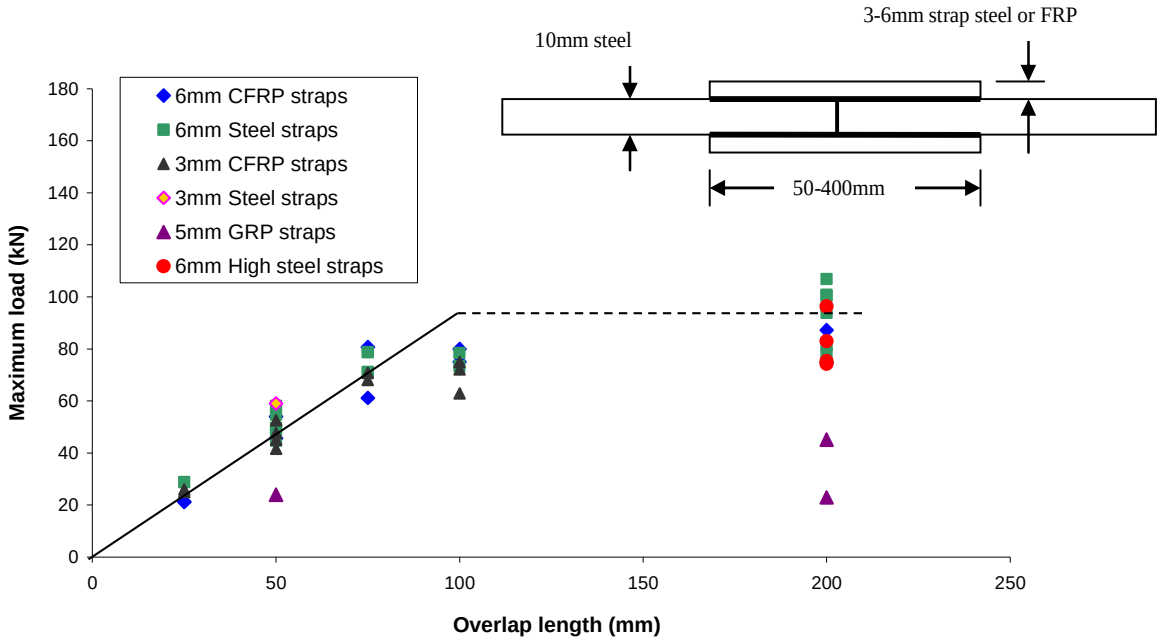

Figure 4. Failure loads of steel/steel and steel/CFRP joints with different overlaps and outer adherends thickness.

- thinner CFRP straps in longer joints exhibits slightly lower strength than equivalent thicker ones

- steel/steel joints with high strength tensile steel show slightly lower strength in comparison with the equivalent joints with low strength steel.

Investigation of the fractured surfaces and joints, especially with long overlaps, suggests that steel/CFRP is failing nearer the interface between the surface ply (0-direction) and resin and the adhesive bondline. This is perhaps due to resin or adhesive failure starting at the middle of the joint. It is also possible that tensile failure of the laminate has occurred where tensile stress exceeded 1000 MPa. The steel/steel joint is failing at the adhesive, but after yielding of the steel itself. The GFRP/steel joints failed at relatively low load at the interface of the resin with adhesive bondline. Figure 5 shows typical failure surfaces and failure modes for different joints.

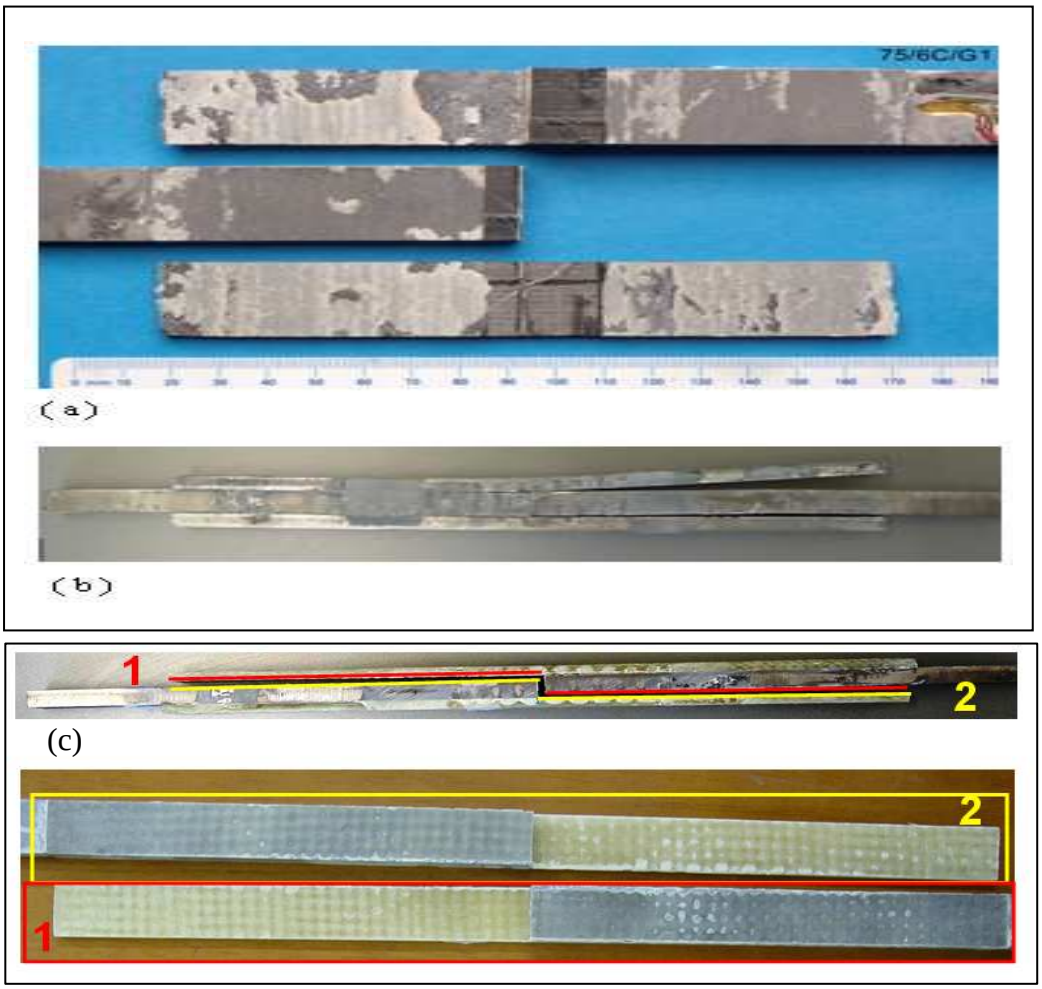

Figure 5. Failure modes and surfaces - (a) 75/6C/G1, (b) 200/6H/G2 and (c) 200/5P/G1.

Imaging systems

In connection with the mechanical testing, both standard low rate (ARAMIS 4M) and high speed (ARAMIS HHS with two Photon APX-RS high speed cameras) digital image correlation (DIC) measurements were carried out at the Technical University of Denmark (DTU) to measure full surface 3-D displacement and 2-D strain fields at the joint while undergoing testing. The standard DIC system operating at 1 frame per second with 4 mega-pixel image resolution was primarily used to capture the deformation of the joint specimen throughout the entire loading history, while the high speed DIC system operating at 3000 frames per second and with maximum 1 mega-pixel resolution captured only the failure incident. Figure 6 (a) shows the system set up in a 155 kN MTS 810 servo-hydraulic test machine at DTU. Figure 6 (b,c.d)) shows a typical contour of the first principle strain which is plotted for the specimen 200/6C/G1 just prior (c) to and after (d) crack propagation has initiated. The DIC measurements clearly

indicate for this specimen that propagation failure is starting at the centre of the specimen propagating towards the strap/joint ends.

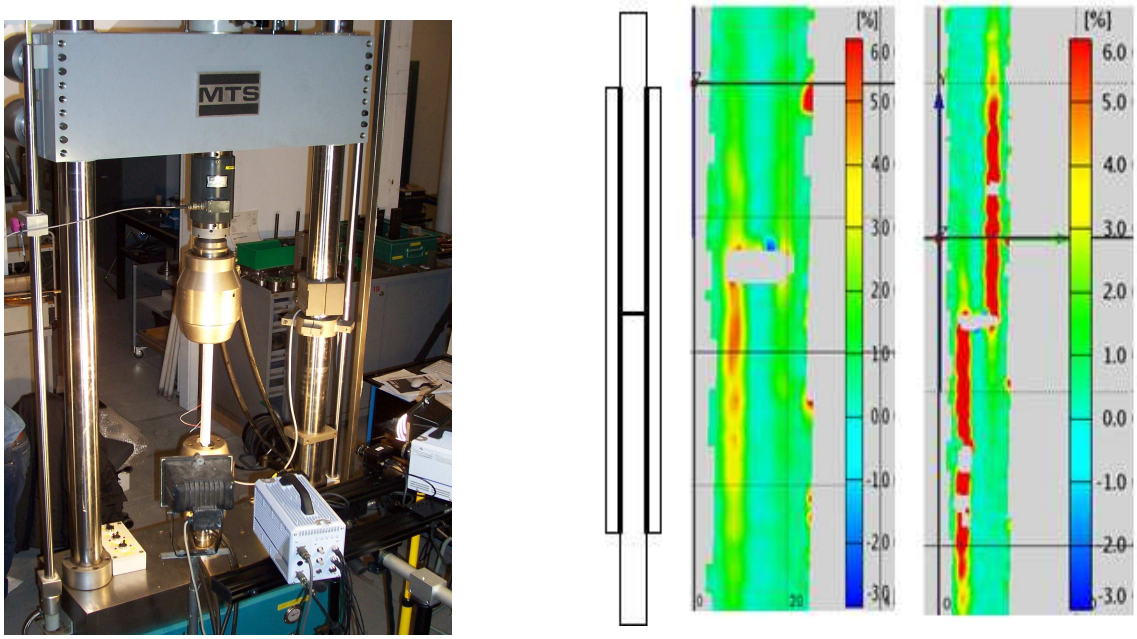

(a) (b) (c) (d)

Figure 6. DIC measurement systems at DTU and major principal strain measurements - (a) system's set up, for (b) long specimen 200/6C/G1, (c) failure initiating and (d) damage propagation along the adhesive bondlines.

NUMERICAL MODELLING

The finite element analysis (FEA) in this section is focused on CFRP/steel specimens (models) designated 25/6C/G1, 50/6C/G2, 100/6C/S1 and 200/6C/G1. 2-D non-linear models were constructed in ABAQUS (as well as other software) using eight-noded solid quadrilateral plane strain elements (as well as others). The boundary conditions, loading and mesh methodology are shown in Figure 7. The 0.5 mm adhesive bondline was divided into five layers through thickness with a standardised fine mesh towards the joint ends. This allowed stress and strain data to be taken along paths created at the upper interface of the adhesive with the outer adherend, and at the lower interface of the adhesive with the inner adherend. The nodes on the free surface were ignored due to stress singularity problems which normally occur here. The first point on each path was taken at 0.05 mm in from the free edge. In a similar fashion the 0.1 mm matrix resin adjacent to the adhesive bondline was modelled into two layers to account for stress details within the resin. The material properties used for the analyses are based on the values from Table 1. These were obtained from various sources including manufacturers and laboratory tests. The steel and adhesive adherends were modelled as elasto-plastic. The composite was modelled as an elastic isotropic layer. The 6 mm CFRP adherend is modelled into up to 12 layers representing plies at 0/90. The plies were separated by 0.1 mm matrix resin. In some cases the whole composite was treated as one isotropic material with average Young's modulus. The two cases (Figure 7) seem to give little difference in the overall behaviour of the joints within the elastic limits. However, in order to study the localised stresses it was necessary to have something in between. Therefore it was decided that only the first two plies at 0/90 sequence were modelled into layers while the rest of the composite (outer adherend) was modelled as a bulk isotropic material.

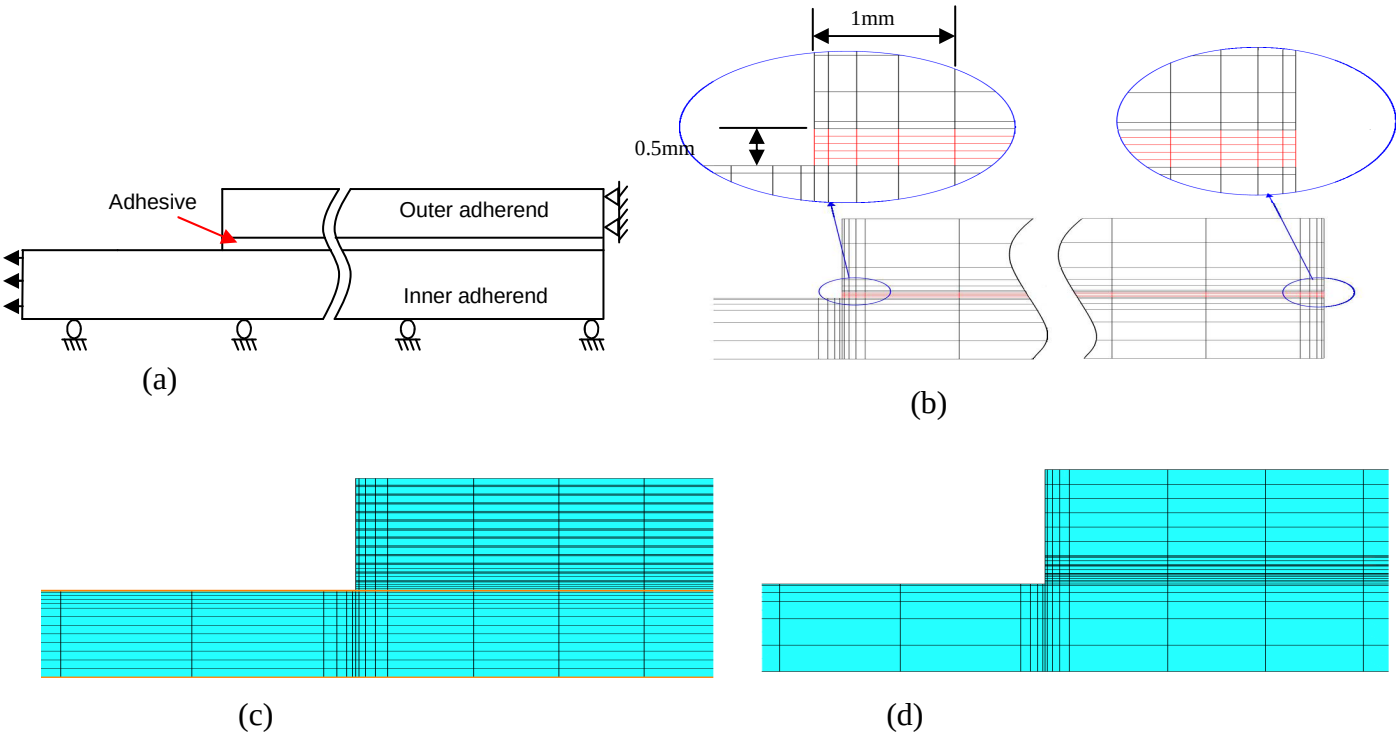

Figure 7. FEA modelling for DLS joints – (a) loading and boundary conditions, (b) standardisation of mesh, (c) 12 layers outer adherend/CFRP and (d) 3 layers outer adherend/CFRP.

Table 1. Materials properties

Property		GFRP WR	Polyester resin	CFRP	Epoxy resin	Adhesive	Steel
Young's modulus [GPa]	E11	25.5	3.6	126.3	4	1.8	210
	E22	5.8	-	5.5	-	-	-
Shear modulus [GPa]	G12	3.1	-	3.3	-	-	-
Poisson's ratio	υ12	0.15	0.35	0.3	0.38	0.36	0.3
	υ21	0.15	-	0.0131	-	-	-
Tensile strength [MPa]		300	26	1400	65	40	395
Shear strength [MPa]		62	-	137.2	-	26	-

The validation of the numerical models showed good correlation between the experimental and numerical strain values at the corresponding locations (see Figure 3). Figure 8 compares the results for models 50/6C/G2 and 200/6C/G1. The former was modelled as multiple composite layers while the latter assumed average properties for the CFRP. In fact both models gave reasonable agreements, especially within the elastic limits of the adherends. The property of the steel in the long overlap seems to be more difficult to correlate (SG2). Therefore, a more detailed

steel property is needed. In addition the experimental curve for the long overlap, is showing nonlinearity also for the CFRP after 70 kN load for the 200/6C/G1.

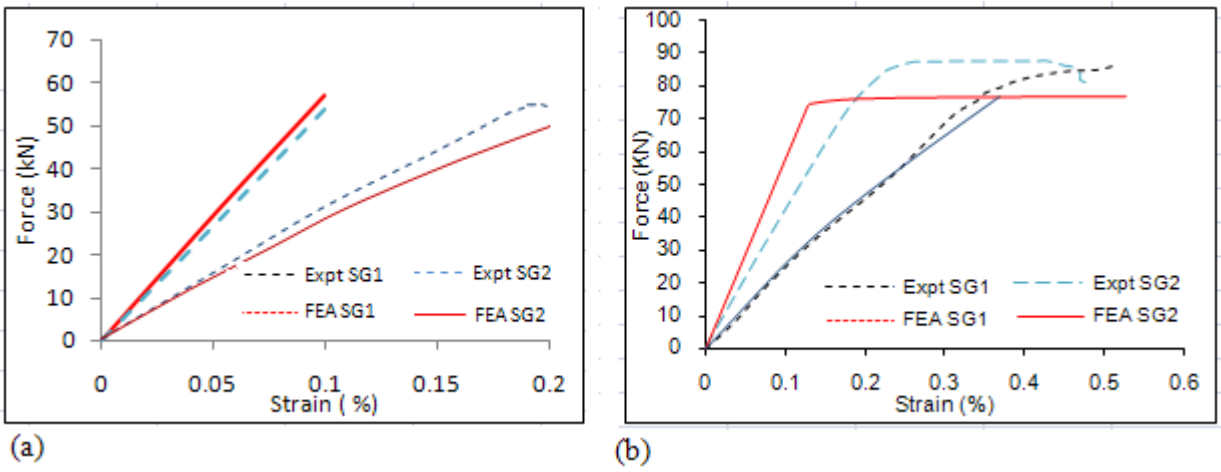

Figure 8. Correlation of force/strain curves-(a) specimen 50/6C/G2 and (b) specimen 200/6C/G1.

Figure 9 shows adhesive stresses distributions along the joint at the interface with the inner and outer adherends, for the 50 mm overlap. The maximum principal (PS) stresses are as expected high nearer the edge of the joints and tend to be higher at the right hand side of the joint (upper interface). Also, the adhesive seems to reach full plasticity in shear. Besides these critical stresses within the adhesive, the figure (c) shows another critical location which is the resin at the interface with the adhesive to the right hand side/centre of the joint. The stress contour shows a very high level of principal stress for the brittle epoxy resin which could be the mean source of failure initiation and propagation. The tensile strength of the matrix epoxy resin is 65 MPa, as given by the manufacturer (see Table 1).

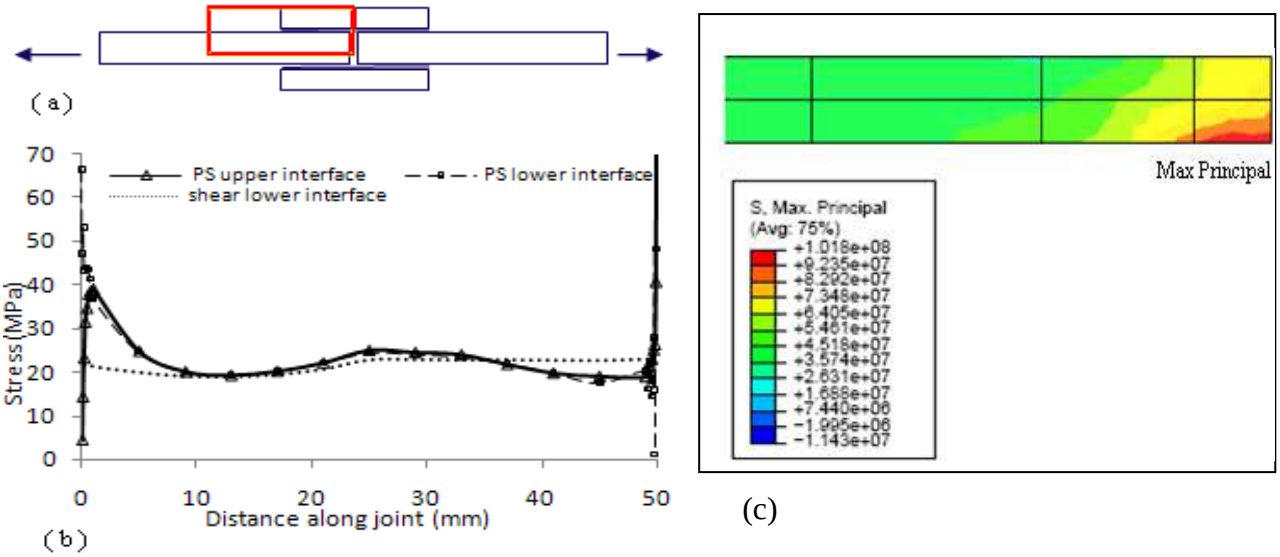

Figure 9. Stresses in steel/CFRP model/joint 50/6C/G2 - (a) stresses location, (b) stresses distribution along upper adhesive interface and (c) contour of maximum principal stress in the first resin layer.

In order to determine the critical stresses, it was necessary to carry out check of various locations within the models. Figure 10 shows such locations for a CFRP/steel model. The following stresses and locations were considered:-

- shear and peel stresses at the upper adhesive interface with top resin (RHS)
- tensile stress at the top resin interface with the adhesive bondline (RHS)
- tensile stress at 0-direction top CFRP ply (RHS)
- tensile stress of inner steel adhernd (LHS)

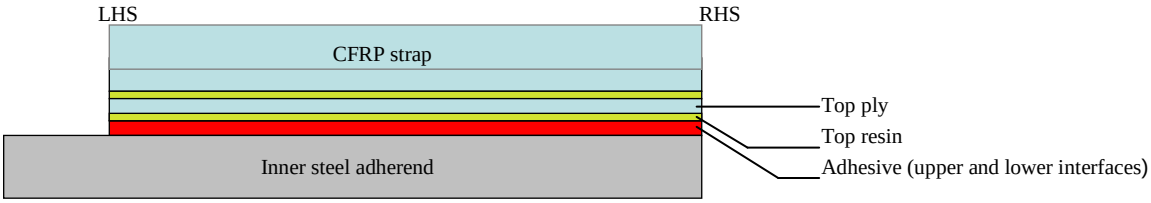

Figure 10. Possible failure initiation locations within the steel/CFRP DLS models.

The level of these critical stresses help to predict joint failure, but with a large margin of error. Furthermore, what was critical for short overlaps may not be so for longer ones. Principal or tensile stresses of the top epoxy resin layer seem to give good indication of joint failure. The scatter among the models is about 30%.

Another important approach to predict failure is the level of plastic shear stress within the adhesive. Figure 11 shows the stress distributions along the upper interface of the adhesive with the CFRP laminate (outer adherend). All three steel/CFRP models exhibited similar peel and principal stresses at the joint ends, especially at the right hand side of the joint. The 50 mm overlap seemed to produce a largely plastic behaviour and interestingly both the 100 and 200 mm cases developed a similar size plastic zone, about 40 mm. A possible failure criterion here is that following the plasticity in shear, a brittle fracture can develop leading to steady crack propagation, as idealised in Figure 11(b). This will be discussed further in the following section.

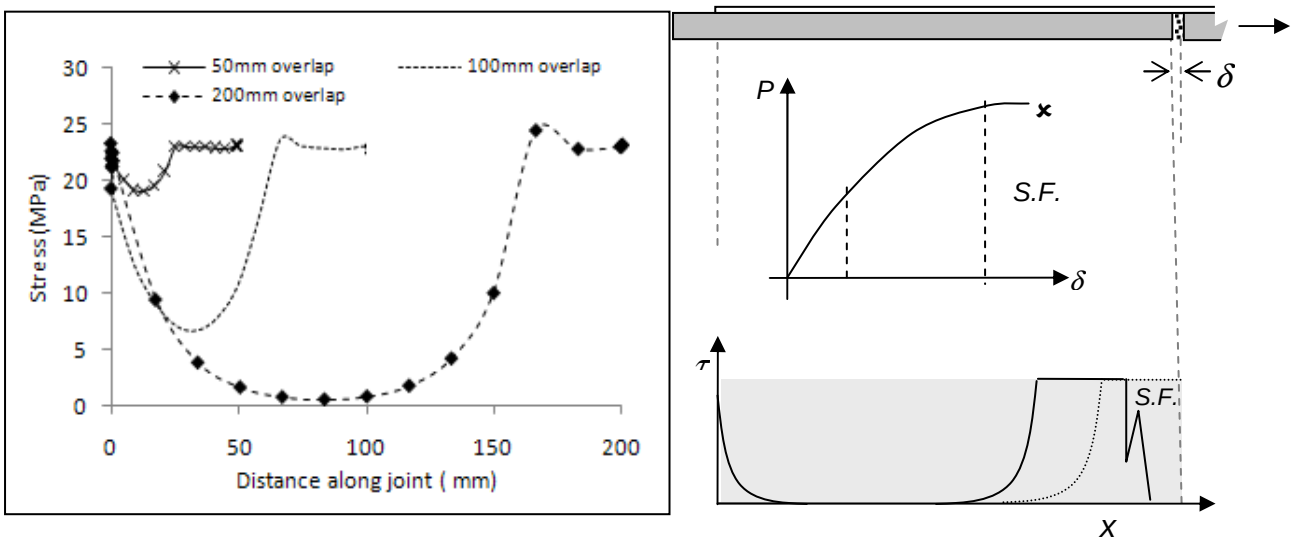

Figure 11. (a) Shear stress distributions along the upper interface of the 50/6C/G2, 100/6C/S1 and 200/6C/G1 models and (b) idealisation of shear stress distribution showing a stable fracture (S.F) zone.

DISCUSSION

The standard fabrication method used in this study can be adopted for practical application and the test results from fabricated specimens suggest the bonding process is robust. However, some

joints, especially long ones, showed some scatter and this applies to both steel/steel and steel/CFRP specimens. The steel/steel case displayed highest strength. The test results for long overlaps (200 mm) suggest a limited static strength advantage over 100 mm overlap. Results from an intermediate overlap length of 150mm overlap would be useful to confirm this. The shorter overlap joints were able to carry loads up to the level where the entire bondline yielded in shear causing joint fractures. The results from the high strength steel seem to have no advantage in this case. On the contrary some of the low tensile strength steel joints produced higher strength! Therfore, further mechanical testing is required to assess the fabrication process and to understand the joint behaviour and failure.

The FEA strategy of modelling the first two plies of the CFRP and their resin layers seems to yield encouraging results, while accounting for maximum stress and strain values at critical spots, including the matrix resin. The results from both experiments including the DIC system and FEA confirm that failure tends to start at the centre of the DLS joint at the interface between the adhesive and CFRP laminate for the configurations where the inner adherend is stiffer than the two outer adherends. The exception is the long steel/steel specimens where the combined stiffness of the outer adherends is larger than that of the inner adherend such that the largest load transfer through the bondline occurs at the free ends of the outer adherends to the left hand side of the joint. In those cases, the fracture started from the free ends of the overlaps (i.e. from the left).

The FEA results which are based on critical stress or strain values at prescribed distances from critical locations are a useful tool to predict joint failure, especially for short overlaps. This approach however, gave inconsistent results and this made it difficult to predict joint failure for models with long overlaps. An alternative is offered by modelling the fracture specifically. The basic assumption of this approach is that final fracture of the bondline occurs at the applied loading where the energy available to progress the damage exceeds the damage resistance of the bondline (see Figure 11). There are four distinct contributions to the energy balance that may be considered , namely i) the work performed by the externally applied forces , ii) the elastic energy released from the specimen, iii) the work dissipated due to deformations in the bondline and iv) the work of creating the damage to the adhesive bondline. To proceed with this approach it is necessary to establish the distribution of stresses and strains in the adherends and bondline that is reasonably representative of what occurs when the joint is loaded up to its capacity. For simple joint geometries, it is possible to establish simple formulae for the stresses and strains leading to simple formulas for the energy contributions. Simple formulae for the fracture load of some simple joint geometries have been formulated by McGeorge [6]. They account for the elastic energy in the adherends and adhesive as well as for the inelastic dissipation of energy in the bondline. The same approach may be applied to DLS joint geometries. A complication is that two distinct fracture modes are possible with this joint geometry and both need to be considered. Work is in progress to derive the simple formulae for the case with long overlaps. Implementation in numerical tools would require a damage model. A bi-linear traction-separation law for a cohesive zone model (CZM) [7] or similar damage models could be an option.

Key conclusions from this study include; (i) the initial work showed a limited advantage in using high strength steel for long overlaps although this may change with a higher strength adhesive; (ii) CFRP composite provides double the joint strength of the equivalent GRP within steel/composite joints; (iii) the overlap plateau for the tested steel and CFRP joints appears to be limited to 100 mm, under quasi-static loading; (iv) a considerable length of the bondline was loaded into the inelastic range before fracture, typically up to 50 mm for joints with high failure load, carrying much of the applied loading, thus showing that attempts at predicting failure of such joints would have to account for nonlinear inelastic adhesive behaviour; (v) various failure

criteria can be used for long overlaps, but perhaps fracture of the bondline after it is partially plasticised is the way forward.

ACKNOWLEDGEMENT

This work has been performed within the context of the Network of Excellence on Marine Structures (MARSTRUCT) partially funded by the European Union through the Growth Programme under contract TNE3-CT-2003-506141.

REFERENCES

1. Echtermeyer, A.T., McGeorge, D., Sund, O.E., Anderson, H.W., Fischer, K.P. (2005). Repair of FSPO with Bonded Composite Patches. Fourth international conference on composite materials for offshore applications. Houston, TX. CEAC.

2. Hashim, S. A., Knox, E.M. (2004), Aspect of Joint evaluation in thick-adherend applications, The J. Adhesion, 80, 569-583, 2004.

3. Potter, K.D., Guild, F.J., Harvey, H.J., Wisnom, M.R., Adams, R.D. (2001). Understanding and control of adhesive crack propagation in bonded joints between carbon fibre composite adherends I. Experimental. International Journal of Adhesion and Adhesives. pp 435-443.

4. Richardson, G., Crocombe, A.D., Smith, P.A. (1995) Failure prediction in adhesives joints by various techniques including the modelling of crack development. Proc SAEIV, Bristol 1995 p44-50.

5. Zhu Y and Kedward K (2005), 'Methods of Analysis and Failure Predictions for Adhesively Bonded Joints of Uniform and Variable Bondline Thickness', *DOT/FAA/AR-05/12*, Washington DC, Office of Aviation Research.

6. McGeorge D (2009), Inelastic fracture of adhesively bonded overlap joints. Eng Fracture Mech, submitted for publication.

7. Crocombe, A.D., Graner Solana, A., Abdel Wahab, M.M., Ashcroft, I.J., Fatigue behaviour in adhesively-bonded single lap joints, Proc. Science and Technology of Adhesion and Adhesives, Oxford September 2008, p187-190.